Biochemistry

pubs.acs.org/biochemistry Article

Electrostatic Contribution to ^{19}F Chemical Shifts in Fluorotryptophans in Proteins

Michael Maxwell,[‖] Yi Jiun Tan,[‖] Richmond Lee, Thomas Huber, and Gottfried Otting*

Cite This: *Biochemistry* 2023, 62, 3255−3264 Read Online

ACCESS | Metrics & More | Article Recommendations | Supporting Information

ABSTRACT: DFT calculations indicate that the ^{19}F chemical shifts of aromatic rings containing single fluorine substituents are sensitive to the electric fields and electric field gradients at the position of the fluorine atom. The present work explores whether long-range structure restraints can be gained from changes in ^{19}F chemical shifts following mutations of charged to uncharged residues. ^{19}F chemical shifts of fluorotryptophan residues were measured in two different proteins, GB1 and the NT* domain, following mutations of single asparagine residues to aspartic acid. Four different versions of fluorotryptophan were investigated, including 4-, 5-, 6-, and 7-fluorotryptophan, which were simultaneously installed by cell-free protein synthesis using 4-, 5-, 6-, and 7-fluoroindole as precursors for the tryptophan synthase present in the S30 extract. For comparison, the ^{1}H chemical shifts of the corresponding nonfluorinated protein mutants produced with ^{13}C-labeled tryptophan were also measured. The results show that the ^{19}F chemical shifts respond more sensitively to the charge mutations than the ^{1}H chemical shifts in the nonfluorinated references, but the chemical shift changes were much smaller than predicted by DFT calculations of fluoroindoles in the electric field of a partial charge in vacuum, indicating comprehensive dielectric shielding by water and protein. No straightforward correlation with the location of the charge mutation could be established.

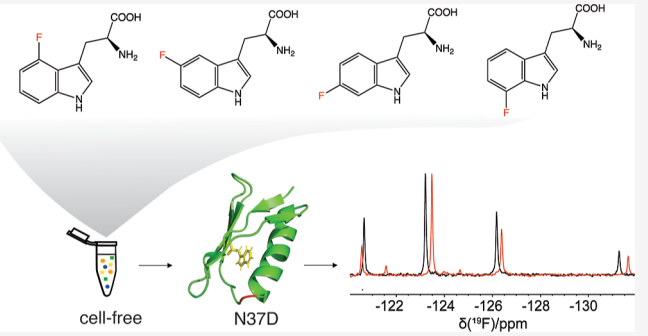

INTRODUCTION

Through-space electrostatic interactions have been identified as dominant contributors to ^{19}F chemical shifts, with electric field-induced shifts predicted to be on the order of 10 ppm.[1] At the atomic level, the ^{19}F chemical shifts of carbon-bonded fluorine correlate with computed polarization charge densities, which also predict the capacity of the organic fluorine to act as a hydrogen-bond acceptor.[2] Experimentally, ^{19}F chemical shift changes of up to 19 ppm have been reported for fluorinated ligands binding next to the charged phosphoserine residue in the active site of phosphoglucomutase.[3] Using computations of electric fields and electric field gradients combined with molecular dynamics, Warshel and co-workers succeeded in predicting the relative ^{19}F chemical shifts of five 5-fluorotryptophan residues in *Escherichia coli* galactose binding protein with good accuracy.[4] These results suggest that the change in ^{19}F chemical shift in response to the mutagenesis of an uncharged for a charged residue presents information about the direction and magnitude of the electrostatic field at the site of the ^{19}F spin, and this effect could act over relatively long distances as electrostatic fields decrease more slowly with distance than, e.g., magnetic dipole−dipole interactions. Fluoroaromatics are expected to respond to electric fields with particularly high sensitivity due to their high polarizability.[5]

Notably, however, Gerig and co-workers pointed out that ^{19}F chemical shifts can be predicted with similar accuracy by stressing the van der Waals contribution to shielding.[6] Subsequent calculations of the ^{19}F chemical shifts of the five 6-fluoroptryptophan residues in *E. coli* dihydrofolate reductase further highlighted the importance of short-range interactions but also the difficulty to compute ^{19}F chemical shifts sufficiently and accurately to assign the ^{19}F-NMR spectrum.[7] Subsequently, molecular dynamics were shown to be of critical importance for the calculation of ^{19}F chemical shift tensors and average chemical shifts by quantum mechanical calculations.[8,9] In summary, it is generally accepted that short-range contacts and electric field effects are significant determinants for ^{19}F chemical shifts of the same amino acid type in a protein, whereas the contribution of long-range electrostatic field effects is relatively small.[10,11] The low sensitivity of ^{19}F chemical shifts toward surface charges is anecdotally underpinned by the observation that acetylation of the side chain

Received: August 3, 2023
Revised: September 29, 2023
Accepted: October 18, 2023
Published: November 7, 2023

https://doi.org/10.1021/acs.biochem.3c00408
Biochemistry 2023, 62, 3255−3264

Scheme 1. Chemical Structure of (a) 4-Fluorotryptophan, (b) 5-Fluorotryptophan, (c) 6-Fluorotryptophan, and (d) 7-Fluorotryptophan

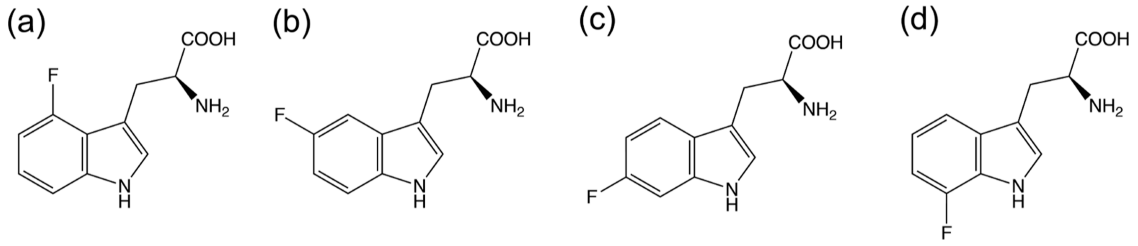

(a)

MHHHHHHGGSENLYFQGSHTTPWTNPGLAENFMNSFMQGLSSMPGFTASQLDKMSTI
AQSMVQSIQSLAAQGRTSPNDLQALNMAFASSMAEIAASEEGGGSLSTKTSSIASAM
SNAFLQTTGVVNQPFINEITQLVSMFAQAGMNDVSA

(b)

MASMTGMTYKLILNGKTLKGETTTEAVDAATAEKVFKQYANDNGVDGEWTYDDATKT
FTVTEENLYFQGHHHHHH

Figure 1. Amino acid sequences of the reference protein constructs. His_6 tags are highlighted in bold; TEV cleavage sites are underlined, and mutation sites are highlighted in bold and underlined. (a) NT* domain construct. The numbering in the crystal structure 4FBS[17] refers to the tryptophan residue as residue 10. (b) GB1 construct. The numbering in the crystal structure 2QMT[18] refers to the tryptophan residue as residue 43.

amino groups of lysine in hen egg white lysozyme caused only very small changes in ^{19}F chemical shifts of 4-fluorotryptophan and 4-fluorophenylalanine.[12] Furthermore, changes in ^{19}F chemical shifts in response to changes in pH were limited to 1.4 ppm or less, which is sizable but significantly smaller than the spectral range of ^{19}F NMR signals observed.[13] The relatively small impact of surface charges can be attributed to the dielectric properties of water and protein, along with counterions associated with the ionized side chains, which are expected to shield the electric fields.

Chemical shift changes of the order of 1 ppm are readily measured, and this prompted us to measure the difference in ^{19}F chemical shifts between proteins with and without a point mutation that introduces a charge site-specifically. It is well-known that charged residues in the core of a protein can destabilize its 3D structure and therefore charged residues usually are solvent-exposed in wild-type proteins.[14] To minimize structural perturbations, we changed single asparagine residues to aspartate, formally changing no more than an NH_2 group into an oxygen atom while, at neutral pH, adding a negative charge. By making Asp/Asn mutations on the surface of the protein, we speculated that the short lengths of the side chains of Asp and Asn would limit the degree of electrostatic shielding by hydration water molecules.

We selected two proteins, GB1 and the NT* domain,[15] which contain single buried tryptophan residues, and substituted the tryptophan residue by 4-, 5-, 6-, and 7-fluorotryptophan (in the following abbreviated as 4FW, 5FW, 6FW, and 7FW, respectively; Scheme 1). The C−F bonds of 4FW and 7FW point in opposite directions, and the same change in the electric field may be expected to change the ^{19}F chemical shifts in opposite directions.

EXPERIMENTAL PROCEDURES

Construct Design. The reference construct of the monomeric NT* domain comprised an N-terminal His_6 tag followed by a TEV cleavage site (Figure 1A).[15] Five mutation sites were selected for the NT* domain, and the following mutations were made: S22N, S22D, Q53N, Q53D, T61N, T61D, L90D, L90N, T121N, and T121D. The DNA sequences encoding each NT* domain mutation were designed and purchased from Twist Bioscience (USA) and cloned into a pCDF vector.[16] Each NT* domain mutant was PCR-amplified from the plasmid template, and the amplicon was purified using a gel extraction kit (Isolate III PCR and gel kit, Bioline/meridian Bioscience, USA). Eight-nucleotide single-stranded overhangs were generated as described previously for use in continuous-exchange cell-free protein synthesis (CFPS).[17]

The reference construct of GB1 comprised GB1 fused to the expression peptide MASMTG followed by a C-terminal TEV cleavage site and a His_6 tag (Figure 1B). Ten mutation sites were selected for GB1, and the following mutations were made: N8D, T17N, T17D, T25N, T25D, Q32N, Q32D, Q32E, D36N, N37D, D40N, E42N, E42D, D46N, and D47N. Wild-type GB1 was cloned into a pETMSCI plasmid,[18] and this was used as a template to generate point mutations via overlap PCR with mutation primers. The PCR-amplified mutant genes were generated, purified, and assembled with eight-nucleotide single-stranded overhangs for CFPS as described above for the NT* domain mutants. All GB1 primers and gene fragments were purchased from Integrated DNA Technologies (USA). In the following, the amino acid sequences of the reference constructs are referred to as the wild type.

Protein Production and Purification. All NT* domain and GB1 proteins were produced by CFPS from PCR-amplified DNA. The CFPS reactions were performed following an established protocol.[21] The CFPS reactions were conducted at 30 °C for 16 h using 1 mL of inner reaction mixture and 10 mL of outer buffer. Tryptophan was omitted from the mixture of amino acids and substituted with either double-labeled $^{13}C/^{15}N$ tryptophan at a final concentration of 0.1 mM or 4-,

https://doi.org/10.1021/acs.biochem.3c00408
Biochemistry 2023, 62, 3255−3264

5-, 6-, and 7-fluoroindole (each at a final concentration of 0.25 mM) as precursors for the in vitro production of 4FW, 5FW, 6FW, and 7FW by the tryptophan synthase present in the S30 extract.[22] The fluoroindoles were first added individually for the wild-type NT* domain and GB1 production to assign the ^{19}F chemical shifts. The subsequent samples of the NT* domain and GB1 mutants were produced using a mixture of fluoroindoles in each reaction.

Following the CFPS reaction, the inner reaction mixture was collected and centrifuged at 13,000 rpm at 4 °C for 60 min. The supernatant was loaded onto a 1 mL Ni-NTA column (GE Healthcare, USA), equilibrated with buffer A (50 mM Tris−HCl, 350 mM NaCl, 10 mM imidazole, and 5% glycerol, pH 7.5). The column was washed with 30 column volumes of buffer A and the protein eluted with buffer B (same as A but with 500 mM imidazole). The eluted protein was concentrated and washed by ultrafiltration using Amicon Centricon concentrators (Millipore, USA) with a molecular weight cutoff of 3 kDa. Protein yields were 1.5−3 mg/mL for both fluorotryptophan and ^{15}N/^{13}C-Trp-labeled NT* domain mutants and 0.3−0.6 mg/mL for GB1 containing fluorotryptophans and 2−3 mg/mL for ^{15}N/^{13}C-Trp-labeled GB1.

The His_6 purification tag was removed from all mutants using TEV cleavage. TEV cleavage reactions were performed at 4 °C overnight in 5 mL of reaction buffer (50 mM Tris−HCl, 100 mM NaCl, 1 mM DTT, pH 7.5) at a 1:20 TEV to fusion protein ratio. After TEV cleavage, the liberated proteins were isolated by passing the reaction mixture through a 1 mL Ni-NTA column (GE Healthcare, USA) equilibrated with reaction buffer and collecting the flow through. The NT* domain and GB1 mutants were concentrated and buffer-exchanged into NMR buffer I (50 mM Tris−HCl, 100 mM NaCl, 30 μM TFA, 10% D_2O, pH 7.5) and NMR buffer II (20 mM MES, 100 mM NaCl, 100 μM TFA, 10% D_2O, pH 6.5), respectively. After the protein concentration and buffer exchange, each sample was analyzed by mass spectrometry and NMR spectroscopy.

Mass Spectrometry. Intact protein analysis was performed by using an Orbitrap Elite Hybrid Ion Trap-Orbitrap mass spectrometer connected to an UltiMate 3000 UHPLC instrument (Thermo Scientific, USA). 0.1% formic acid and an acetonitrile gradient (10−85%) were used to inject the samples into the mass analyzer via an Agilent ZORBAX SB-C3 Rapid Resolution HT Threaded Column. Data were collected in positive ion mode by using an electrospray ionization source. The Xtract function in the Qual Browser software tool of Xcalibur (version 3.0.63) was used to deconvolute and determine the protein intact mass.

NMR Spectroscopy. All spectra were recorded at 25 °C. 1D ^{19}F NMR data were recorded on a Bruker AVANCE 600 MHz NMR spectrometer equipped with a 5 mm TCI cryoprobe with an inner coil tunable to ^{19}F. Samples were in 5 mm NMR tubes at 50−400 μM concentrations. All ^{19}F NMR spectra used an acquisition time of 45 ms and a total recording time between 1 and 14 h depending on sample concentration. The spectra were calibrated relative to the ^{19}F NMR signal of TFA (−75.5 ppm).

^{13}C-HSQC spectra were recorded on a Bruker AVANCE III 800 MHz NMR spectrometer equipped with a 5 mm TCI cryoprobe. ^{13}C-HSQC spectra were recorded with t_{1max} = 5.8 ms and t_{2max} = 70.1 ms using a total recording time of 1.3 h per experiment. A TOCSY-relayed ^{13}C-HSQC experiment (TOCSY mixing time 20 ms) was performed to assign the ^{13}C−^{1}H groups of the tryptophan side chains.

The chemical shifts were measured using CcpNmr AnalysisAssign (version 3.1.1).[23]

DFT Calculations of ^{19}F Shielding. The effect of point charge perturbing ^{19}F chemical shifts in fluoroindoles was calculated using Gaussian16.[24] The isotropic magnetic shielding tensors of the ^{19}F spin of fluoroindoles in the gas phase were determined by DFT calculations using the gauge-independent atomic orbital method[25] and at B3LYP/6-31+G(d,p) level of theory.[26] Calculations with no charge served as the reference for calculations with a point charge of +0.5 positioned between 3 and 15 Å from the ^{19}F spin on the lines orthogonal and parallel to the C−F bond of the fluoroindoles.

RESULTS

Protein Production and NMR Resonance Assignment. Samples of GB1 and the NT* domain were successfully prepared with 4-, 5-, 6-, and 7-fluorotryptophan by CFPS in a dialysis system,[21] substituting tryptophan in the reaction by a mixture of the four different fluorotryptophan versions. Typical protein yields were 0.3−3 mg per mL cell-free inner reaction mixture in 10 mL of outer buffer, using 1.3 mg fluoroindoles. Mass spectrometric analysis of the NT* domain samples showed that at most 25% of the NT* domain contained tryptophan instead of fluorotryptophan, while the GB1 mutants contained negligible amounts of tryptophan (Figures S1 and S2).

The efficiency with which different fluorotryptophan isomers were incorporated into the proteins varied. In the NT* domain, 6FW was incorporated most efficiently, whereas the largest signal in the ^{19}F NMR signal of GB1 was from 5FW. 7FW was incorporated least well, suggesting lower conversion rates of 7-fluoroindole to 7FW by the tryptophan synthase. Quadrupling the amount of 7-fluoroindole increased the incorporation of 7FW into GB1 (Figure S3). Expression experiments conducted with the NT* domain showed improved expression yields with 0.25 mM concentration of each of the fluoroindoles than with 4-fold larger fluoroindole concentrations, indicating some inhibitory effects associated with the fluoroindoles or fluorotryptophans.

The ^{19}F NMR signals of the four different versions of fluorotryptophan were assigned by preparing four different samples of the wild-type proteins with 4FW, 5FW, 6FW, or 7FW (Figures S4 and S5). Between the two proteins, the ^{19}F chemical shifts varied between 0.5 and 6 ppm, whereas the ^{1}H chemical shifts of the natural tryptophans differed by not much more than 0.5 ppm (Figures S6 and S7). This demonstrates the high sensitivity of the ^{19}F chemical shifts toward effects other than ring currents from other aromatic residues in the core of the protein, which play a predominant role for ^{1}H chemical shifts. The NMR signals of the different fluorotryptophan isomers were readily resolved in the 1D ^{19}F NMR spectra, and any changes in chemical shifts induced by subsequent mutations were too small to affect the resonance assignments (Figures 2 and 3).

To compare the size of chemical shift changes observed in the ^{19}F NMR spectra with those observed for protons in the corresponding positions in natural tryptophan, we also produced samples of all mutants with ^{13}C-labeled tryptophan instead of fluorotryptophan and measured the ^{1}H chemical shift changes in the ^{13}C-HSQC spectra. The ^{1}H NMR signals of the reference (wild-type) constructs containing ^{13}C-labeled

https://doi.org/10.1021/acs.biochem.3c00408
Biochemistry 2023, 62, 3255−3264

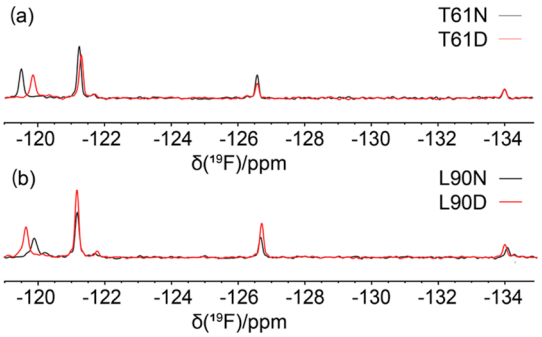

Figure 2. ^{19}F NMR spectra of mutant NT* constructs produced with a mixture of 4FW, 5FW, 6FW, and 7FW. The NMR spectra of the constructs containing either Asn or Asp are plotted in black and red, respectively. The assignment is (low-field to high-field) 4FW, 6FW, 5FW, and 7FW (Figure S4). For comparison, the ^{19}F chemical shifts of the free amino acids in methanol have been reported as −122.0 (6FW), −123.8 ppm (4FW), −125.1 ppm (5FW), and −135.2 ppm (7FW).[27]

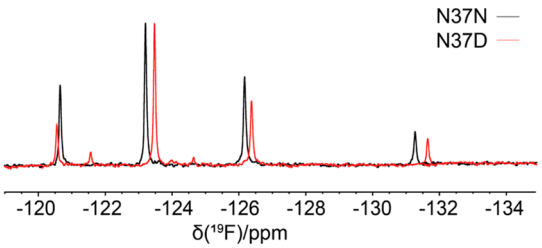

Figure 3. ^{19}F NMR spectra of GB1 produced with a mixture of 4FW, 5FW, 6FW, and 7FW. The black spectrum is of the reference construct (also referred to as wild type) containing Asn in position 37, and the red spectrum is of the mutant N37D. The assignment is (low-field to high-field) 6FW, 5FW, 4FW, and 7FW (Figure S5).

tryptophan were assigned by a ^{13}C-HSQC spectrum with a TOCSY relay (Figures S6 and S7).

To obtain a significant set of data, the sites selected for mutation comprised not only Asn residues present in the wild-type proteins but also other sites, which were first mutated to Asn before mutation to Asp.

Chemical Shift Changes in Response to Mutations. In the NT* domain, the ^{19}F chemical shifts of 4FW were more sensitive to mutations than those of 5FW, 6FW, or 7FW (Figure 4a). This pattern was not observed in the GB1 domain (Figure 5a). Inspection of the crystal structure of the monomeric NT domain (PDB ID 4FBS)[19] reveals that changing the $C^{\varepsilon 3}H$ group of Trp10 in the crystal structure to a C−F group would result in an intraresidual interatomic H^{α}−F distance of only 1.8 Å (compared with 2.0 Å for the corresponding H^{α}−$H^{\varepsilon 3}$ distance in the wild-type protein), whereas the crystal structure can accommodate the fluorine atom of 5FW, 6FW, and 7FW without major van der Waals clashes. This suggests that the extraordinarily large chemical shift changes observed for 4FW in the NT* domain, even in response to Asp/Asn mutations more than 20 Å from the fluorine atom, arise from a spring-loaded structure where the 4F-indole ring is in an energetically unfavorable conformation. This may also explain the large downfield shift of the ^{19}F NMR signal of 4FW in the NT* domain compared with GB1 (Figures S4 and S5). In contrast, the conformation of Trp43 in the crystal structure of GB1 (2QMT)[20] indicates the absence of similar van der Waals clashes arising from the fluorine substitutions.

Changes in ^{19}F chemical shifts were observed not only in response to mutations between Asn and Asp residues but also upon mutation of other residue types to Asn or Asp (Figures 4b and 5b). These changes were often larger than those observed for the Asp/Asn switch, as, for example, in the cases of the mutants T61N and T121N in the NT* domain (Figure 4b) and T25N in GB1 (Figure 5b).

There was no obvious way in which either the magnitude or sign of the $\Delta\delta(^{19}F)$ values arising from Asp/Asn switches correlated with the distance of the mutation from the fluorine atom or the direction of the C−F bond relative to the mutation site. For example, $\Delta\delta(^{19}F)$ values of the Asp/Asn switch in GB1 with 4FW and 7FW were of the same sign for the N40D and N37D mutants (Figure 5a), although the C−F bonds in 4FW and 7FW point in opposite directions. Similarly, the sign of the $\Delta\delta(^{19}F)$ value differed between the N36D and N37D mutants for the 6FW and 7FW mutants (Figure 5a), although these mutations involved sequentially neighboring residues close to each other. In the case of the NT* domain, L90 is about 20 Å from the indole ring of Trp10 (Figure 6), but its mutation still generated significant chemical shift changes in the ^{19}F-NMR spectrum (Figure 4a,b). In the ^{1}H NMR spectrum of the mutants produced with ^{13}C-Trp, the corresponding $\Delta\delta(^{1}H)$ values were generally less significant (Figure 4c,d), suggesting that the chemical shift changes were not simply a consequence of a change in ring currents due to small conformational changes in the core of the protein. In summary, ^{19}F generally displayed larger chemical shift changes than ^{1}H, but they cannot be interpreted in simple terms that would allow derivation of structural restraints.

Sensitivity of Chemical Shift Changes to Shielding by Salt or Water. To explore the sensitivity of the ^{19}F chemical shifts to long-range electrostatic fields, we also measured the ^{19}F NMR spectra of some of the NT* domain mutants with increased concentrations of NaCl. At high salt (200 versus 100 mM NaCl), the $\Delta\delta(^{19}F)$ values measured for Asp/Asn switches changed only a little, even increasing in magnitude for 7FW in the mutants at positions 53 and 90 (Table S7). This indicates that counterions associated with Asp residues did not significantly contribute to electrostatic shielding.

The possibility of electrostatic charges being shielded by hydration water was explored by comparing the ^{19}F chemical shift changes effected by a Glu/Gln switch with those of an Asp/Asn switch in position 32 of GB1. At this site, the $\Delta\delta(^{19}F)$ values associated with the Asp/Asn switch agreed with the expectation that the change in ^{19}F chemical shift elicited by the electric field of the new carboxylate is greatest, if the field aligns with the C−F bond, changes sign for different C−F bond directions, and is more pronounced for shorter fluorine−carboxylate distances and much smaller or negligible if the C−F bond is perpendicular to the vector connecting the ^{19}F spin with the carboxylate. As expected for more complete shielding associated with the greater solvent exposure of the carboxylate group attached to the longer side chain, smaller $\Delta\delta(^{19}F)$ values were measured for the Glu/Gln switch than for the Asp/Asn switch. Unexpectedly, however, $\Delta\delta(^{19}F)$ of 5FW changed the sign between the Glu/Gln and Asp/Asn mutants (Table S8). It thus appears that while long-range electrostatic fields contribute to ^{19}F chemical shift changes, other effects can be just as large.

https://doi.org/10.1021/acs.biochem.3c00408
Biochemistry 2023, 62, 3255−3264

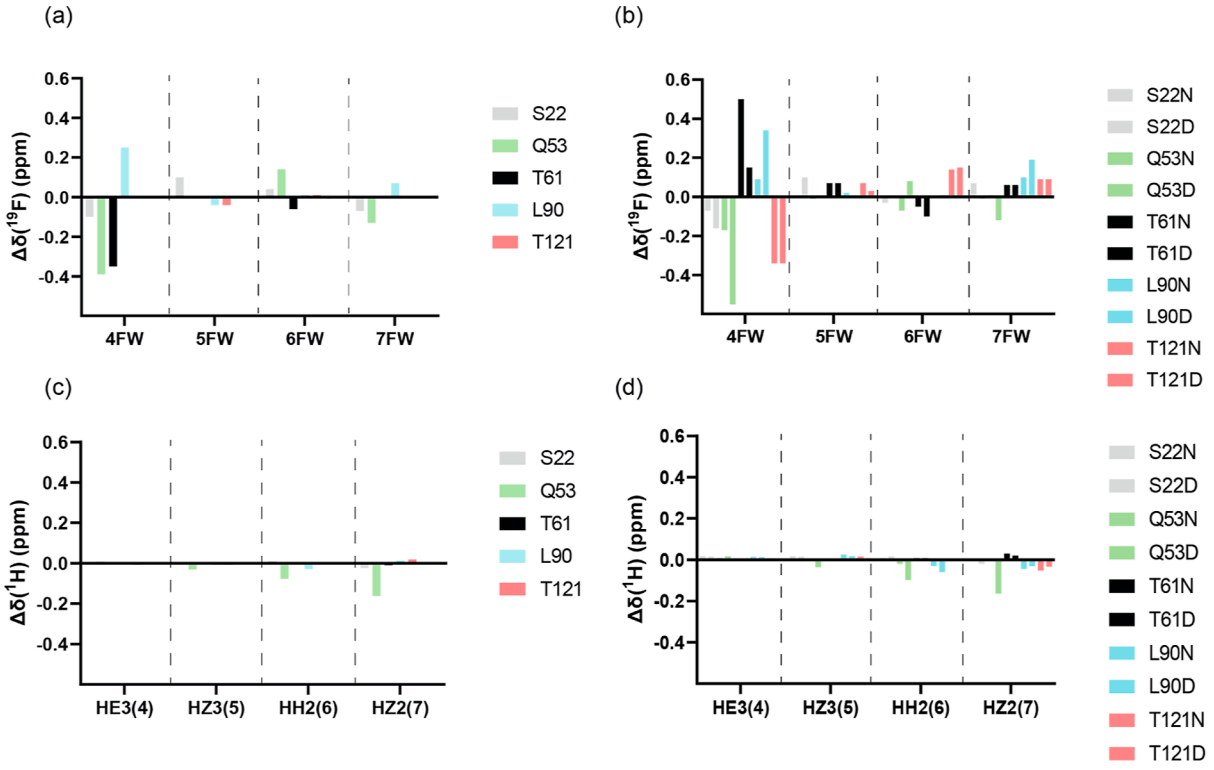

Figure 4. Chemical shift changes of the ^{19}F NMR signals of fluorotryptophans and ^{1}H NMR signals of tryptophan in response to mutations of solvent-exposed amino acids in the NT* domain. The spectral data are shown in Figures S8 and S10. (a) ^{19}F chemical shift changes of 4-,5-, 6-, and 7-fluorotryptophan. $\Delta\delta(^{19}F)$ is the chemical shift observed with aspartate minus the chemical shift observed with asparagine at the mutation sites indicated. (b) Same as (a) but for mutations at sites that are neither aspartate nor asparagine in the wild-type protein. $\Delta\delta(^{19}F)$ is the chemical shift observed with Asn or Asp at the mutation sites indicated minus the chemical shift observed for the reference protein containing the wild-type residue. (c) Same as (a) but for ^{1}H chemical shift changes of ^{13}C-labeled tryptophan. The positions $H^{\varepsilon 3}$, $H^{\zeta 3}$, $H^{\eta 2}$, and $H^{\zeta 2}$ correspond to the positions 4, 5, 6, and 7, respectively, of the indole ring. (d) Same as (b) but for ^{1}H chemical shift changes of ^{13}C-labeled tryptophan.

Indirect Effects. Besides a redistribution of counterions around the protein, the change in the electric field associated with an Asp/Asn switch alters the conformational preferences of other amino acid side chains. For example, introducing an Asp residue at position 53 of the NT* domain introduces a negative charge in the proximity of the side chain of Glu17, which is not engaged in a salt bridge. The ensuing electrostatic repulsion may explain why the Asp/Asn switch in position 53 elicited the largest chemical shift changes both in the ^{19}F and ^{1}H NMR spectra (Figure 4a,c). In the case of GB1, the crystal structure shows the indole ring of Trp43 in close contact with most of the side chain of Lys31, which forms a salt bridge with Glu57 (Figure 7). Due to its close proximity to the indole ring, a small relocation of the amino group of Lys31 arising from altered electrostatics could potentially affect the ^{19}F chemical shifts of fluorotryptophans more strongly than any Asp/Asn switch at a greater distance. To assess this hypothesis, the mutant K31 M was investigated with the Asp/Asn switch at position 32. Regardless of whether position 31 featured a lysine or methionine residue, $\Delta\delta(^{19}F)$ values changed in the same direction and by similar magnitudes (Figure 8 and Table S9). This suggests that the conformation of Lys31 and the position of its side chain amine are not easily perturbed by installing a negatively charged carboxylate at a distance of about 10 Å.

Conversely, the ^{1}H chemical shifts of Trp10 in the NT* domain were most significantly perturbed by an Asp/Asn switch in position 53 (Figure 4c). The perturbation was particularly pronounced for the $H^{\zeta 2}$ atom, although it is almost 4 Å further from the Asp/Asn switch site than the $H^{\varepsilon 3}$ atom of the same indole ring. The ^{19}F chemical shift changes of the corresponding FW mutants were also relatively large but did not change in the same direction (Figure 4a). This makes it difficult to interpret the chemical shift changes as a conserved small structural change in response to the mutation. Notably, position 53 is near Glu17 and a repulsive interaction with Asp53 may cause some structural adjustment. Importantly, other Asp/Asn switches barely changed the ^{1}H chemical shifts of the tryptophan ring, whereas ^{19}F chemical shifts changed, highlighting the universally greater sensitivity of ^{19}F chemical shifts.

Interestingly, except for mutations in position 53 in the NT* domain, the ^{19}F chemical shift change observed for an Asp mutant relative to the wild type was always in the same direction as the change observed for the corresponding Asn mutant (Figures 4b and 5b). In other words, the change in charge, as affected by an Asp/Asn switch, affected the ^{19}F chemical shifts less than the change in steric demand by mutations of different amino acid side chains. The ^{19}F spin thus appears exquisitely sensitive to changes in steric demand transmitted from the mutation site by an allosteric pathway of small conformational adjustments throughout the protein, ultimately responding to a very small change in the local environment. Even after discounting the chemical shift changes of 4FW in the NT* domain and those arising from an Asp/Asn switch in position 53, it is difficult to attribute the measured ^{19}F chemical shift changes solely to changes in the electric charge of solvent-accessible amino acids.

https://doi.org/10.1021/acs.biochem.3c00408
Biochemistry 2023, 62, 3255−3264

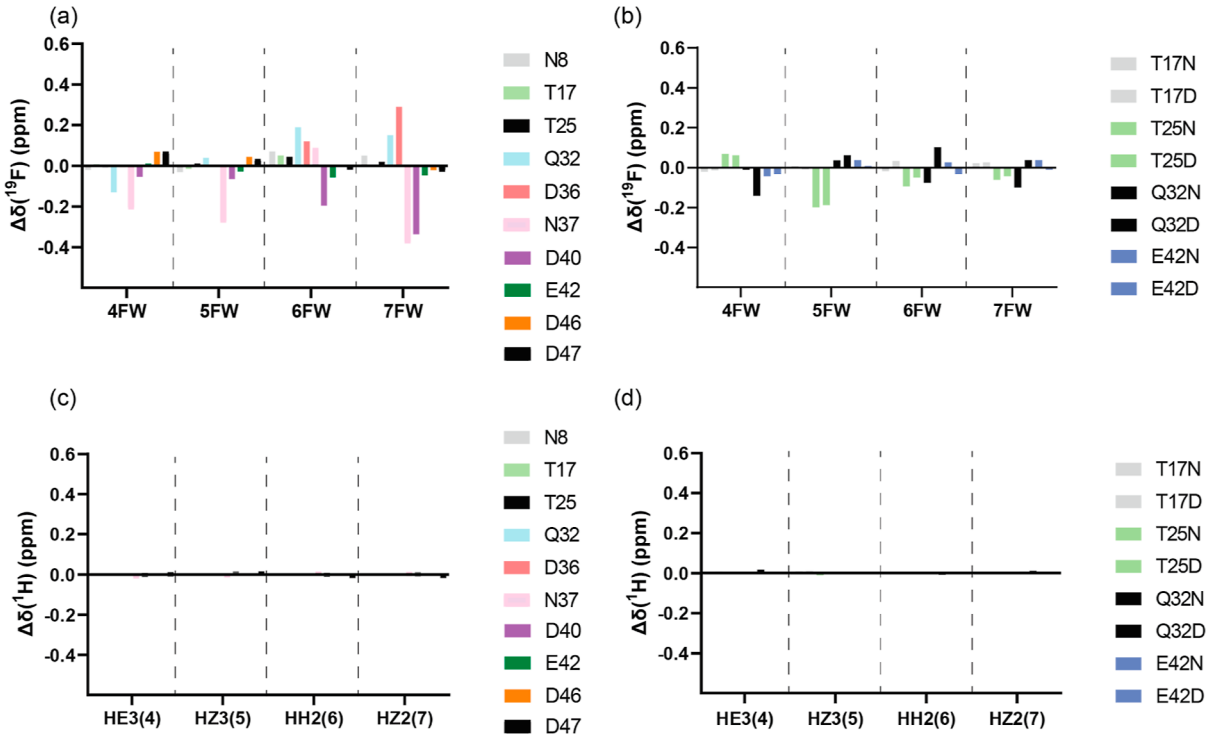

Figure 5. Chemical shift changes of the ^{19}F NMR signals of fluorotryptophans and ^{1}H NMR signals of tryptophan in response to mutations of solvent-exposed amino acids in GB1. See Figure 4 for the naming conventions used and the calculation of $\Delta\delta(^{19}F)$ and $\Delta\delta(^{1}H)$. The spectral data are shown in Figures S9 and S11. (a) ^{19}F chemical shift changes of 4-, 5-, 6-, and 7-fluorotryptophan. (b) Same as (a) but for mutations at sites that are neither aspartate nor asparagine in the wild-type protein. (c) Same as (a) but for ^{1}H chemical shift changes of ^{13}C-labeled tryptophan. (d) Same as (b) but for ^{1}H chemical shift changes of ^{13}C-labeled tryptophan.

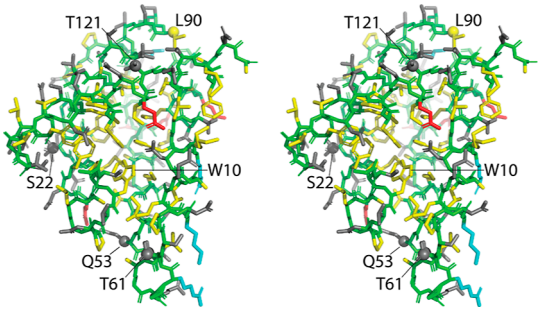

Figure 6. Stereoview of the crystal structure 4FBS of the monomeric NT domain mutant A72R.[17] In the NT* domain, the potential dimer interface is stably disrupted by the mutations D40K and K65D.[15] Color code: backbone, green; negatively charged side chain, red; positively charged side chain, blue; hydrophobic side chain, yellow; and hydrophilic side chain, gray. Spheres identify the β-carbons of residues mutated in the present work. A cartoon representation is shown in Figure S12a.

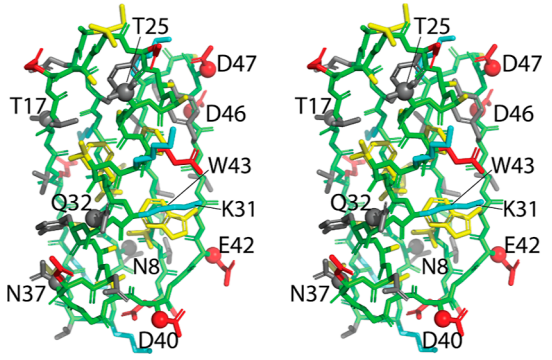

Figure 7. Stereoview of the crystal structure 2QMT of GB1.[18] See Figure 6 for the color code used. Balls identify the β-carbons of amino acids mutated in the present work. A cartoon representation is shown in Figure S12b.

Theoretical Prediction of Charge Effects on ^{19}F Chemical Shifts. To gain insights into the magnitude of ^{19}F chemical shift changes that can be expected from a charge near a ^{19}F spin in fluorotryptophan, DFT calculations were performed on 4F-indole, 5F-indole, 6F-indole, and 7F-indole in vacuum. A point charge of +0.5 was positioned on an axis aligned with the C−F bond, and the distance r between the fluorine atom and the charge increased stepwise. Figure 9 plots the predicted change in the ^{19}F chemical shift with increasing distance. The simulations suggest that even a half-charge located 12 Å from the ^{19}F spin can easily change the chemical shift by 1 ppm. Clearly, the charge effect predicted by the calculations defines only an upper limit as protein cores possess a finite electric susceptibility that shields the electric field. Fits to the data are approximately proportional to r^{-2}. The different fluoroindoles responded to the charge differently, with 4FW showing the smallest effect and 6FW showing the largest effect.

DFT calculations with the half-charge positioned on axes perpendicular to the C−F bond predict a smaller response of the ^{19}F chemical shift. Defining a coordinate system with the origin at the ^{19}F spin, the z-axis along the C−F bond, the y-axis perpendicular to the plane of the indole, and the x-axis in the plane of the indole (Figure S13a), the change in shielding affected by the charge positioned on the y axis is about a third of the effect on the z axis (Figure S13b), and the effect of a

https://doi.org/10.1021/acs.biochem.3c00408
Biochemistry 2023, 62, 3255−3264

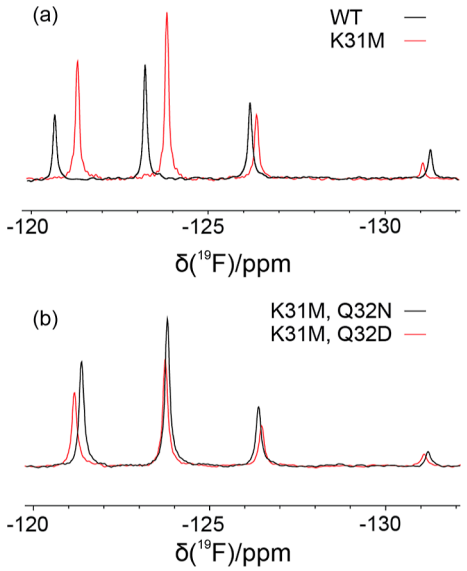

Figure 8. 1D ^{19}F NMR spectra of the GB1 K31M mutant produced with a mixture of 4FW, 5FW, 6FW, and 7FW. (a) Overlay of the ^{19}F NMR spectra of the reference construct referred to in this work as wild-type (black) and mutant GB1 K31M (red). (b) ^{19}F NMR spectra of the GB1 K31M construct with additional mutations Q32N (black) and Q32D (red).

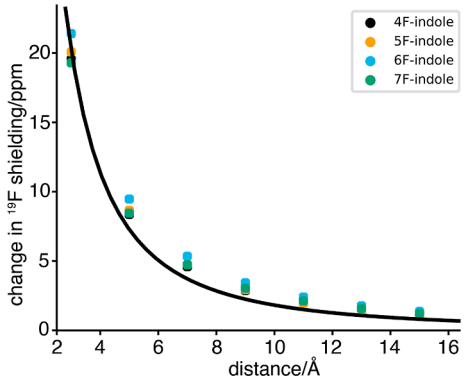

Figure 9. Calculated change in the ^{19}F chemical shift due to an electric charge (+0.5) at different distances from the ^{19}F spin in different fluoroindoles. The DFT calculations are for the molecules in vacuum with the charge located on the axis defined by the C−F bond. The black curve corresponds to a quadratic decay.

charge in the *x* direction is also relatively small (Figure S13c). The magnitude of the predicted effects was much greater than reported by the experimental data, indicating that the fluorotryptophan residues are effectively shielded from the electrostatic field of carboxyl groups on the protein surface.

Using the DFT calculations to estimate the effect of the Asp/Asn switches in GB1 and the NT* domain on the ^{19}F chemical shifts of the fluorotryptophan residues delivered no significant correlation with the experimental data (Figure S14).

DISCUSSION

Protein Expression, Yield, and ^{19}F Spectral Resolution. The present work demonstrates that all four fluorotryptophan versions (4FW, 5FW, 6FW, and 7FW) can readily be produced simultaneously from the corresponding fluoroindoles in a CFPS system based on *E. coli* S30 extract. The yields of incorporation are high (>85% in the case of the NT* domain, almost complete in the case of GB1), but the different fluoroindoles are processed with different rates, with 7FW incorporated least efficiently. The different incorporation rates facilitate tracking of the four ^{19}F NMR signals in response to mutations. The ^{19}F NMR signals of the four fluorotryptophan variants were readily resolved in the 1D ^{19}F NMR spectra.

The NT* domain used in this work is the D40K/K65D double mutant of the NT domain. This charge reversal prevents dimerization of the protein even at low pH.[15,28] The sites selected for Asp and Asn mutations in the present work were outside the dimer interface of the NT domain.

The GB1 construct used in the present work was preceded by the first six codons of the T7 gene 10 to enhance the protein expression yields.[29] The codons translate into the hexapeptide MASMTG, which assumes a flexible conformation. Our CFPS conditions resulted in incomplete cleavage of the N-terminal methionine residue (Figure S2), but this heterogeneity did not translate into visibly heterogeneous ^{19}F NMR spectra.

Chemical Shift Changes in Response to Mutations. As expected, the ^{19}F chemical shifts of the fluorotryptophan residues in GB1 and the NT* domain proved to be sensitive reporters of small changes in the proteins. The present work was primarily concerned with the response of the ^{19}F chemical shifts of fluorotryptophan residues in the protein core to changes in the electric field produced by installing a new negative charge on the protein surface. We reasoned that a buried fluorotryptophan residue would sense the electric field from the carboxylate group with little shielding by salt and hydration water as the side chains of aspartate and asparagine are short. In this way, long-range structural information could be encoded in ^{19}F chemical shift changes associated with an Asp/Asn switch at a solvent-exposed site. An Asp/Asn switch at a solvent-exposed site is readily achieved by site-directed mutagenesis and minimally alters the chemical structure of the protein as the switch formally involves no more than the change of a negatively charged oxygen atom for a neutral NH_2 group. According to the 3D structures of the wild-type NT* domain and GB1, no hydrogen-bond donor was within reach of any of the fluorine atoms in any of the fluorotryptophan versions, excluding the possibility that changes in the ^{19}F chemical shift arise from changes in H-bonds with fluorine. The structure of GB1 also reports no hydrogen bond with the side chain of Trp43, whereas the structure of the NT* domain shows a hydrogen bond between the indole NH of Trp10 and the side chain carbonyl oxygen of Asn70. In the case of 5-fluoroindole and 5FW, H-bond formation with the indole NH has been shown to alter the ^{19}F chemical shift.[30,31] Therefore, if the mutations of the NT* domain changed the H-bond character of the indole NH, this could have contributed to the observed changes in the ^{19}F chemical shifts.

Regardless of the origin in ^{19}F chemical shift changes, our results confirm that an Asp/Asn switch as far as 20 Å from the site of a fluorotryptophan residue can cause a measurable change in the ^{19}F chemical shift. Furthermore, every single mutation tested changed the ^{19}F chemical shift measurably in at least two of the four fluorotryptophan versions. Regarding the same mutations, ^{1}H chemical shifts of natural tryptophan were generally far less responsive (see, e.g., Table S6).

Quantitative comparisons with ^{1}H chemical shift changes are compromised by the greater length of a C−F versus C−H bond and the larger van der Waals radius of fluorine versus hydrogen, and this is expected to cause minor adaptations of

https://doi.org/10.1021/acs.biochem.3c00408
Biochemistry 2023, 62, 3255−3264

the protein structure when tryptophan is replaced by fluorotryptophan. Conceivably, any slight conformational adjustment of the aromatic rings in the core of GB1 and the NT* domain in response to a surface mutation would be subtly different in the proteins containing fluorotryptophan compared with those containing natural tryptophan. Very small conformational adjustments of aromatic amino acids present a plausible mechanism for transmitting the effect of mutations on the protein surface to the tryptophan residue in the core of the protein, and this effect may explain the small ^{1}H chemical shift perturbations observed for natural tryptophans following mutation of a single solvent-exposed residue, as observed even in GB1 which is a highly stable single-domain protein.

It is also conceivable that allosteric effects are amplified by local van der Waals constraints created by the greater space requirements of a C−F versus C−H group. For example, the unusually large ^{19}F chemical shift changes observed for 4FW in the NT* domain (Figure 4) arguably arise from an intraresidue van der Waals clash that is not a concern for natural tryptophan.

Electric Field Effects. The changes in the ^{19}F chemical shifts observed upon switching from an aspartate to an asparagine residue were smaller than anticipated. DFT calculations of fluoroindoles in vacuum predicted that a single charge significantly changes the ^{19}F chemical shift (Figure 9), and the large differences in ^{19}F chemical shifts observed between fluorotryptophans in GB1 and the NT* domain confirm the outstanding sensitivity of the ^{19}F chemical shift as a reporter of the chemical environment. Similar magnitudes of ^{19}F chemical shift changes have been calculated for 3-fluorotyrosine interacting with ions and polar as well as nonpolar atoms, with positive and negative charges showing opposite effects.[32] In the present work, however, we were unable to detect sizable effects arising from the change of a single surface charge. In fact, the chemical shift perturbations resulting from mutation between two uncharged residues were usually greater than the chemical shift changes associated with the Asp/Asn switches. This indicates that any long-range effect from the electrostatic field generated by a solvent-exposed carboxylate is small. Electric fields may still be decisive for the ^{19}F chemical shifts as, arguably, the small conformational changes that are manifested in the chemical shift perturbations observed in the ^{1}H NMR spectra of natural tryptophan residues could also alter local electric fields and field gradients in subtle ways.

The DFT calculations of the ^{19}F chemical shift of fluoroindoles in a vacuum were performed to gain an impression of the magnitude of the effect that a charge could have and any dependence on its location relative to the indole ring system. The prediction is that a charge positioned on the axis defined by the C−F bond approximately changes the ^{19}F chemical shift with increasing distance r approximately in proportion to r^{-2}, with easily measurable effects 15 Å and further from the ^{19}F spin. While it proved difficult to establish experimental evidence for this effect, it could be concealed in multiple ways, including the complexity of protein structures, the unknown structural response of the protein structures to the mutations, and the unknown capacity of protein and hydration water molecules to shield the electric field. To explain why experiments with high versus low salt concentrations and a Glu/Gln versus Asp/Asn switch did not yield clear patterns of ^{19}F chemical shift changes, we speculate that the switches may rearrange the preferential orientations of charged amino acid side chains and any salt bridges on the protein surface. As a knock-on effect, counterions may be redistributed. A redistribution of charges would change the electrostatic field in the core of the protein in a way different from the simple addition of a point charge.

In GB1, the side chain of Lys31 is in intimate contact with the tryptophan side chain and its charged amine group is highly solvent-exposed. Reasoning that a small relocation of this close amine group in response to Asp/Asn switches could cause outsized ^{19}F chemical shift perturbations, we investigated the Asp/Asn switch in position 32 of the K31Mmutant. The response of the ^{19}F chemical shifts in these double mutants remained qualitatively the same (Table S9), speaking against major redistributions of charges on the protein surface in response to this Asp/Asn switch.

Finally, we note that ^{19}F chemical shifts can follow trends counter to intuition that only considers inductive effects. For example, the ^{19}F chemical shifts in low-molecular-weight difluorophenyl compounds in $CDCl_3$ were found to correlate with the Hammett constants of substituents in a remote phenyl ring, where through-space effects from electron-withdrawing substituents result in increased ^{19}F shielding.[33,34] Reverse effects such as this can be explained by paramagnetic contributions arising from the coupling of occupied orbitals to unoccupied orbitals and require DFT calculations for quantification.[35] This greatly complicates the interpretation of the ^{19}F chemical shifts.

CONCLUSIONS

The current work shows that proteins with fluorotryptophans can readily be produced from 4-, 5-, 6-, and 7-fluoroindoles in a one-pot cell-free reaction. The ^{19}F NMR signals of all four fluorotryptophan species are well-resolved in the 1D NMR spectra. Our experiments show that the mixture of fluorotryptophans offers a sensitive way of detecting subtle changes in the protein environment at greater distances by maximizing the chance of observing measurable chemical shift changes. As the spectral ranges of different fluorotryptophans overlap,[36−38] the utility of the approach will be greatest for proteins with a single tryptophan residue. Finally, the small response of the ^{19}F chemical shift to altered surface charges implies that surface charges can be neglected when attempting to assign ^{19}F NMR spectra of buried fluorotryptophan residues by comparison to the predictions from DFT calculations.

ASSOCIATED CONTENT

Supporting Information

The Supporting Information is available free of charge at https://pubs.acs.org/doi/10.1021/acs.biochem.3c00408.

Mass spectra of NT* domain mutants with fluorotryptophan; mass spectra of GB1 mutants made with fluorotryptophan; ^{19}F NMR of wild-type GB1 made with mixtures of 4FW, 5FW, 6FW, and 7FW; ^{19}F NMR of NT* domain produced with different individual fluorotryptophans; ^{19}F NMR of GB1 produced with different individual fluorotryptophans; ^{13}C-HSQC with TOCSY relay for assignment of the tryptophan indole protons in the NT* domain; ^{13}C-HSQC with TOCSY relay for assignment of the tryptophan indole protons in GB1; ^{19}F NMR of different Asp/Asn switches in the NT* domain; ^{19}F chemical shift changes in response to Asp/Asn switches in the NT* domain; ^{19}F chemical shift

https://doi.org/10.1021/acs.biochem.3c00408
Biochemistry 2023, 62, 3255−3264

changes in response to mutations to Asp or Asn in the NT* domain; ^{1}H chemical shift changes of tryptophan ring protons in response to mutations to Asp or Asn in the NT* domain; ^{19}F NMR of different Asp/Asn switches in GB1; ^{19}F chemical shift changes in response to Asp/Asn switches in GB1; ^{19}F chemical shift changes in response to mutations to Asp or Asn in GB1; ^{1}H chemical shift changes of tryptophan ring protons in response to mutations to Asp or Asn in GB1; ^{19}F chemical shift changes in the NT* domain in response to Asp/Asn switches at different salt concentrations; ^{19}F chemical shift changes in response to a Glu/Gln switch in GB1 compared with the corresponding Asp/Asn switch; ^{19}F chemical shift changes in response to the Asp/Asn switch in position 32 of wild-type GB1 and GB1 K31M; ^{13}C-HSQC spectra of ^{13}C/^{15}N labeled tryptophan in NT* domain mutants; ^{13}C-HSQC spectra of ^{13}C/^{15}N labeled tryptophan in GB1 mutants; cartoon drawings of the crystal structures of the NT* domain and GB1; calculated effect of an electric charge on ^{19}F shielding; and correlation of predicted and experimental ^{19}F chemical shift changes effected by Asp/Asn switches (PDF)

Accession Codes

NT-domain: Q05H60; GB1: P19909.

AUTHOR INFORMATION

Corresponding Author

Gottfried Otting − *Australian Research Council Centre of Excellence for Innovations in Peptide and Protein Science, Research School of Chemistry, Australian National University, Canberra 2601 Australian Capital Territory, Australia;* orcid.org/0000-0002-0563-0146; Phone: +61 2 61256507; Email: Gottfried.otting@anu.edu.au

Authors

Michael Maxwell − *Australian Research Council Centre of Excellence for Innovations in Peptide and Protein Science, Research School of Chemistry, Australian National University, Canberra 2601 Australian Capital Territory, Australia*

Yi Jiun Tan − *Australian Research Council Centre of Excellence for Innovations in Peptide and Protein Science, Research School of Chemistry, Australian National University, Canberra 2601 Australian Capital Territory, Australia*

Richmond Lee − *School of Chemistry and Molecular Bioscience, University of Wollongong, Wollongong 2500 New South Wales, Australia;* orcid.org/0000-0003-1264-4914

Thomas Huber − *Research School of Chemistry, Australian National University, Canberra 2601 Australian Capital Territory, Australia;* orcid.org/0000-0002-3680-8699

Complete contact information is available at: https://pubs.acs.org/10.1021/acs.biochem.3c00408

Author Contributions

‖M.M. and Y.J.T. contributed equally to the work.

Funding

Financial support by the Australian Research Council, including the Centre of Excellence for Innovations in Peptide and Protein Science (CE200100012), a Discovery Project (DP230100079), and a Laureate Fellowship to G.O. (FL170100019) is gratefully acknowledged.

Notes

The authors declare no competing financial interest.

ACKNOWLEDGMENTS

We thank Professor Haibo Yu for helpful discussions.

REFERENCES

(1) Augspurger, J.; Pearson, J. G.; Oldfield, E.; Dykstra, C. E.; Park, K. D.; Schwartz, D. Chemical-shift ranges in proteins. *J. Magn. Reson.* **1992**, *100*, 342−357.

(2) Vulpetti, A.; Dalvit, C. Hydrogen bond acceptor propensity of different fluorine atom types: an analysis of experimentally and computationally derived parameters. *Chem.—Eur. J.* **2021**, *27*, 8764−8773.

(3) Percival, M. D.; Withers, S. G. ^{19}F NMR investigations of the catalytic mechanism of phosphoglucomutase using fluorinated substrates and inhibitors. *Biochemistry* **1992**, *31*, 505−512.

(4) Pearson, J. G.; Oldfield, E.; Lee, F. S.; Warshel, A. Chemical shifts in proteins: a shielding trajectory analysis of the fluorine nuclear magnetic resonance spectrum of the Escherichia coli galactose binding protein using a multipole shielding polarizability-local reaction field-molecular dynamics approach. *J. Am. Chem. Soc.* **1993**, *115*, 6851−6862.

(5) Kitevski-LeBlanc, J. L.; Prosser, R. S. Current applications of ^{19}F NMR to studies of protein structure and dynamics. *Prog. Nucl. Magn. Reson. Spectrosc.* **2012**, *62*, 1−33.

(6) Chambers, S. E.; Lau, E. Y.; Gerig, J. T. Origins of fluorine chemical shifts in proteins. *J. Am. Chem. Soc.* **1994**, *116*, 3603−3604.

(7) Lau, E. Y.; Gerig, J. T. Origins of fluorine NMR chemical shifts in fluorine-containing proteins. *J. Am. Chem. Soc.* **2000**, *122*, 4408−4417.

(8) Sternberg, U.; Klipfel, M.; Grage, S. L.; Witter, R.; Ulrich, A. S. Calculation of fluorine chemical shift tensors for the interpretation of oriented ^{19}F-NMR spectra of gramicidin A in membranes. *Phys. Chem. Chem. Phys.* **2009**, *11*, 7048−7060.

(9) Dietschreit, J. C. B.; Wagner, A.; Le, T. A.; Klein, P.; Schindelin, H.; Opatz, T.; Engels, B.; Hellmich, U. A.; Ochsenfeld, C. Predicting ^{19}F NMR chemical shifts: a combined computational and experimental study of a trypanosomal oxidoreductase-inhibitor complex. *Angew. Chem., Int. Ed.* **2020**, *59*, 12669−12673.

(10) Gerig, J. T. Fluorine NMR of proteins. *Prog. Nucl. Magn. Reson. Spectrosc.* **1994**, *26*, 293−370.

(11) Arntson, K. E.; Pomerantz, W. C. K. Protein-Observed Fluorine NMR: A Bioorthogonal Approach for Small Molecule Discovery: Miniperspective. *J. Med. Chem.* **2016**, *59*, 5158−5171.

(12) de Dios, A. C.; Pearson, J. G.; Oldfield, E. Secondary and tertiary structural effects on protein NMR chemical shifts: an ab initio approach. *Science* **1993**, *260*, 1491−1496.

(13) Lian, C.; Le, H.; Montez, B.; Patterson, J.; Harrell, S.; Laws, D.; Matsumura, I.; Pearson, J.; Oldfield, E. Fluorine-19 nuclear magnetic resonance spectroscopic study of fluorophenylalanine- and fluorotryptophan-labeled avian egg white lysozymes. *Biochemistry* **1994**, *33*, 5238−5245.

(14) Jones, S.; Marin, A.; MThornton, J. Protein domain interfaces: characterization and comparison with oligomeric protein interfaces. *Protein Eng.* **2000**, *13*, 77−82.

(15) Kronqvist, N.; Sarr, M.; Lindqvist, A.; Nordling, K.; Otikovs, M.; Venturi, L.; Pioselli, B.; Purhonen, P.; Landreh, M.; Biverstål, H.; Toleikis, Z.; Sjöberg, L.; Robinson, C. V.; Pelizzi, N.; Jörnvall, H.; Hebert, H.; Jaudzems, K.; Curstedt, T.; Rising, A.; Johansson, J. Efficient protein production inspired by how spiders make silk. *Nat. Commun.* **2017**, *8*, 15504.

(16) van den Elzen, P. J.; Konings, R. N.; Veltkamp, E.; Nijkamp, H. J. Transcription of bacteriocinogenic plasmid CloDF13 in vivo and in vitro: structure of the cloacin immunity operon. *J. Bacteriol.* **1980**, *144*, 579−591.

(17) Wu, P. S. C.; Ozawa, K.; Lim, S. P.; Vasudevan, S.; Dixon, N. E.; Otting, G. Cell-free transcription/translation from PCR amplified DNA for high-throughput NMR studies. *Angew. Chem., Int. Ed.* **2007**, *46*, 3356−3358.
(18) Neylon, C.; Brown, S. E.; Kralicek, A. V.; Miles, C. S.; Love, C. A.; Dixon, N. E. Interaction of the Escherichia coli replication terminator protein (Tus) with DNA: a model derived from DNA-binding studies of mutant proteins by surface plasmon resonance. *Biochemistry* **2000**, *39*, 11989−11999.
(19) Jaudzems, K.; Askarieh, G.; Landreh, M.; Nordling, K.; Hedhammar, M.; Jörnvall, H.; Rising, A.; Knight, S. D.; Johansson, J. pH-dependent dimerization of spider silk N-terminal domain requires relocation of a wedged tryptophan side chain. *J. Mol. Biol.* **2012**, *422*, 477−487.
(20) Frericks Schmidt, H. L.; Sperling, L. J.; Gao, Y. G.; Wylie, B. J.; Boettcher, J. M.; Wilson, S. R.; Rienstra, C. M. Crystal polymorphism of protein GB1 examined by solid-state NMR spectroscopy and X-ray diffraction. *J. Phys. Chem. B* **2007**, *111*, 14362−14369.
(21) Apponyi, M.; Ozawa, K.; Dixon, N. E.; Otting, G. Cell-free protein synthesis for analysis by NMR spectroscopy. *Methods Mol. Biol.* **2008**, *426*, 257−268.
(22) Qianzhu, H.; Abdelkader, E. H.; Herath, I. D.; Otting, G.; Huber, T. Site-specific incorporation of 7-fluoro-L-tryptophan into proteins by genetic encoding to monitor ligand binding by ^{19}F NMR spectroscopy. *ACS Sens.* **2022**, *7*, 44−49.
(23) Skinner, S. P.; Fogh, R. H.; Boucher, W.; Ragan, T. J.; Mureddu, L. G.; Vuister, G. W. CcpNmr AnalysisAssign: a flexible platform for integrated NMR analysis. *J. Biomol. NMR* **2016**, *66*, 111−124.
(24) Frisch, M. J.; Trucks, G. W.; Schlegel, H. B.; Scuseria, G. E.; Robb, M. A.; Cheeseman, J. R.; Scalmani, G.; Barone, V.; Petersson, G. A.; Nakatsuji, H.; Li, X.; Caricato, M.; Marenich, A. V.; Bloino, J.; Janesko, B. G.; Gomperts, R.; Mennucci, B.; Hratchian, H. P.; Ortiz, J. V.; Izmaylov, A. F.; Sonnenberg, J. L.; Williams-Young, D.; Ding, F.; Lipparini, F.; Egidi, F.; Goings, J.; Peng, B.; Petrone, A.; Henderson, T.; Ranasinghe, D.; Zakrzewski, V. G.; Gao, J.; Rega, N.; Zheng, G.; Liang, W.; Hada, M.; Ehara, M.; Toyota, K.; Fukuda, R.; Hasegawa, J.; Ishida, M.; Nakajima, T.; Honda, Y.; Kitao, O.; Nakai, H.; Vreven, T.; Throssell, K.; Montgomery, J. A.; Peralta, J. E.; Ogliaro, F.; Bearpark, M. J.; Heyd, J. J.; Brothers, E. N.; Kudin, K. N.; Staroverov, V. N.; Keith, T. A.; Kobayashi, R.; Normand, J.; Raghavachari, K.; Rendell, A. P.; Burant, J. C.; Iyengar, S. S.; Tomasi, J.; Cossi, M.; Millam, J. M.; Klene, M.; Adamo, C.; Cammi, R.; Ochterski, J. W.; Martin, R. L.; Morokuma, K.; Farkas, O.; Foresman, J. B.; Fox, D. J. *Gaussian 16*, Revision C.01; Gaussian, Inc.: Wallingford, CT, 2016.
(25) Ditchfield, R. Self-consistent perturbation theory of diamagnetism. I. A gauge-invariant LCAO method for N.M.R. chemical shifts. *Mol. Phys.* **1974**, *27*, 789−807.
(26) Saunders, C.; Khaled, M. B.; Weaver, J. D.; Tantillo, D. J. Prediction of ^{19}F NMR chemical shifts for fluorinated aromatic compounds. *J. Org. Chem.* **2018**, *83*, 3220−3225.
(27) Lee, M.; Phillips, R. S. Fluorine substituent effects for tryptophan in ^{13}C nuclear magnetic resonance. *Magn. Reson. Chem.* **1992**, *30*, 1035−1040.
(28) Abelein, A.; Chen, G.; Kitoka, K.; Aleksis, R.; Oleskovs, F.; Sarr, M.; Landreh, M.; Pahnke, J.; Nordling, K.; Kronqvist, N.; Jaudzems, K.; Rising, A.; Johansson, J.; Biverstål, H. High-yield production of amyloid-β peptide enabled by a customized spider silk domain. *Sci. Rep.* **2020**, *10*, 235.
(29) Camaj, P.; Hirsh, A. E.; Schmidt, W.; Meinke, A.; von Gabain, A. Ligand-mediated protection against phase lysis as a positive selection strategy for the enrichment of epitopes displayed on the surface of E. coli cells. *Biol. Chem.* **2001**, *382*, 1669−1677.
(30) Mitsky, J.; Joris, L.; Taft, R. W. Hydrogen-bonded complex formation with 5-fluoroindole. Applications of the pK_{HB} scale. *J. Am. Chem. Soc.* **1972**, *94*, 3442−3445.
(31) Dalvit, C.; Vulpetti, A. Weak intermolecular hydrogen bonds with fluorine: detection and implications for enzymatic/chemical reactions, chemical properties, and ligand/protein fluorine NMR screening. *Chem.—Eur. J.* **2016**, *22*, 7592−7601.
(32) Isley, W. C., III; Urick, A. K.; Pomerantz, W. C. K.; Cramer, C. J. Prediction of ^{19}F chemical shifts in labeled proteins: computational protocol and case study. *Mol. Pharm.* **2016**, *13*, 2376−2386.
(33) Xi, N.; Sun, M.; Lu, Y.; Bai, C. Electrostatic effects on ^{19}F NMR chemical shifts in *N*-phenyl γ-lactam derivatives. *Tetrahedron* **2022**, *113*, 132733.
(34) Lu, Y.; Sun, M.; Xi, N. Effects of fluorine bonding and nonbonding interactions on ^{19}F chemical shifts. *RSC Adv.* **2022**, *12*, 32082−32096.
(35) Dahanayake, J. N.; Kasireddy, C.; Karnes, J. P.; Verma, R.; Steinert, R. M.; Hildebrandt, D.; Hull, O. A.; Ellis, J. M.; Mitchell-Koch, K. R. Progress in our understanding of ^{19}F chemical shifts. *Annu. Rep. NMR Spectrosc.* **2018**, *93*, 281−365.
(36) Lian, C.; Le, H.; Montez, B.; Patterson, J.; Harrell, S.; Laws, D.; Matsumura, I.; Pearson, J.; Oldfield, E. Fluorine-19 nuclear magnetic resonance spectroscopic study of fluorophenylalanine- and fluorotryptophan-labeled avian egg white lysozymes. *Biochemistry* **1994**, *33*, 5238−5245.
(37) Sun, X.; Dyson, H. J.; Wright, P. E. Fluorotryptophan incorporation modulates the structure and stability of transthyretin in a site-specific manner. *Biochemistry* **2017**, *56*, 5570−5581.
(38) Kenward, C.; Shin, K.; Rainey, J. K. Mixed fluorotryptophan substitutions at the same residue expand the versatility of ^{19}F protein NMR spectroscopy. *Chem.—Eur. J.* **2018**, *24*, 3391−3396.

https://doi.org/10.1021/acs.biochem.3c00408
Biochemistry 2023, 62, 3255−3264